Biochemical and Biophysical Research Communications 371 (2008) 315–319

Contents lists available at ScienceDirect

Biochemical and Biophysical Research Communications

journal homepage: www.elsevier.com/locate/ybbrc

Overlapping functions of different dynamin isoforms in clathrin-dependent and -independent endocytosis in pancreatic β cells

Jingze Lu [1], Zixuan He [1], Junmei Fan, Pingyong Xu *, Liangyi Chen *

National Key Laboratory of Biomacromolecules, Institute of Biophysics, Chinese Academy of Science, Datun Road 15#, Beijing 100101, PR China

ARTICLE INFO

Article history:
Received 14 April 2008
Available online 28 April 2008

Keywords:
Clathrin-independent endocytosis
Pancreatic β cells
Dynamin 1
Dynamin 2
RNA interference

ABSTRACT

Previously, we identified a clathrin-dependent slow endocytosis and a clathrin-independent fast endocytosis in pancreatic β cells, both triggered by elevated cytoplasmic Ca^{2+} concentration. In the current study, we attempted to explore the roles of different dynamin isoforms in these endocytotic processes. We first confirmed the existence of both neuron-specific dynamin 1 and ubiquitous dynamin 2 in INS-1 cells using both quantitative RT-PCR and Western blot experiments. By specifically knocking down the endogenous level of either dynamin isoform from INS-1 cells, we showed that dynamin 1 and dynamin 2 simultaneously participate in the clathrin-independent and -dependent membrane retrieval in pancreatic β cells. Transferrin internalization was also inhibited in cells with knock down of both dynamin 1 and dynamin 2. Based on these results, we argue that different dynamin isoforms play overlapping roles in different types of endocytosis.

In neurons and endocrine cells, portions of the plasma membrane are retrieved following two kinetically different endocytic pathways [1,2]: a slow membrane retrieval that is believed to be a clathrin-dependent process and a fast retrieval that is clathrin-independent [3–5]. The identity of this fast endocytosis remains very controversial, and is proposed to be either "kiss and run" or "bulk endocytosis" [4,6–10]. Its physiological significance is also elusive due to a lack of molecular methods to specifically perturb this endocytic pathway.

One crucial component of the endocytic machinery is the protein that injects energy into a lipid–protein system to separate the vesicle from the plasma membrane during scission. Dynamin was first isolated in 1989, and has been known to play this role for more than a decade [11]. It also plays an indispensable role in the clathrin-independent endocytic process in a variety of cells [3–5]. The conventional dynamin superfamily includes three dynamins: a brain-enriched dynamin 1 (Dyn1) that is concentrated in the presynapse, a ubiquitously expressed dynamin 2 (Dyn2) and dynamin 3 (Dyn3) that is found in the testis and post-synaptic locations [12,13]. Therefore, different dynamins may regulate distinct endocytic processes based on their different distribution profiles. In agreement with this hypothesis, Artalejo et al. [11] showed that injection of an antibody against brain-enriched Dyn1 in chromaffin cells exclusively ablated depolarization-induced fast membrane retrieval, while slow, clathrin-dependent endocytosis was specifically inhibited by the intracellular perfusion of a Dyn2 antibody [3]. However, it is unclear whether such distinct functionalities are ubiquitously applicable, since expressing dominant negative forms of either Dyn1 or Dyn2 inhibits clathrin-dependent transferrin internalization in HeLa cells [14]. Moreover, the interpretations of both studies were compromised due to the possibly non-specific effects induced by their manipulations. Therefore, we decided to dissect the function of Dyn1 and Dyn2 in another cell type using more specific RNA interference method.

As an endocrine cell, pancreatic β cells release insulin in response to food uptake and tightly controlled blood glucose, whereas abnormal insulin secretion is associated with both type 1 and type 2 diabetes [15]. In a previous study, we identified two types of endocytosis in pancreatic β cells stimulated by UV flash-photolysis-induced, homogeneous Ca^{2+} elevation. We identified fast endocytosis as a novel clathrin-independent but actin-dependent membrane retrieval process [4]. All dynamins have a proline-rich domain (PRD) that interacts with numerous actin-related proteins [16], and dynamin is a major link between the actin polymerization and the endocytic machinery [17]. It is possible that the dependence of fast endocytosis on actin is due to the different interactions between actin-associated proteins and different domains of either Dyn1 or Dyn2 [18,19]. Therefore, by measuring fast and slow endocytosis in cells in which either of the dynamin isoforms has been knocked down, pancreatic β cells represent an ideal model for us to test this theory.

* Corresponding authors. Fax: +86 10 64888524.
E-mail addresses: pyxu@moon.ibp.ac.cn (P. Xu), chen_liangyi@yahoo.com (L. Chen).
[1] These authors contributed equally to this work.

0006-291X/$ - see front matter © 2008 Elsevier Inc. All rights reserved.
doi:10.1016/j.bbrc.2008.04.077

Materials and methods

Cell culture and transfection. INS-1 insulinoma cells were cultured and transfected as described previously [20]. Seventy-two hours after transfection of shRNA vectors, cells were detached using trypsin–EDTA and transferred onto poly-L-lysine-coated coverslips.

RNA interference. The Dyn1-EGFP and Dyn2-mRFP vectors were obtained as described previously [4]. Small hairpin oligonucleotides (shRNAs) against the heavy chain of Dyn1 and Dyn2 were designed and cloned into the BamHI–HindIII sites of the pRNAT-H1.1/mRFP or pRNAT-H1.1/EGFP vector [21]. We designed four shRNA sequences targeting each gene and selected the most effective ones by Western blotting. They were: GGAAATGGAACGAATTGTG for rat Dyn1, and GTACAAGGATGAAGAGGAA for Dyn2, respectively. Mouse monoclonal antibodies were used against Dyn2 (BD Pharmingen, San Diego, CA), and a rabbit polyclonal antibody was used against Dyn1 (Affinity BioReagents, Golden, CO) in a diluted form (1:500). β-Actin antibody (Sigma, St. Louis, MO, 1:2000) was used as a control. Western blot experiments were conducted as previously described [4].

RNA isolation and quantitative RT-PCR analysis. INS-1 cells, mouse brain and HEK293 cells were homogenized using a Mixer Mill MM 300 (Qiagen, USA). RNA was isolated following the RNeasy mini kit protocols (Qiagen Inc.) and transcribed into single-stranded cDNA using M-MLV reverse transcriptase (Stratagen, USA) with oligo $(dT)_{18}$ primers (Sangon, Shanghai, China). Real-time PCR analysis was performed using an MX-3000P Real-time PCR Instrument (Stratagen, USA) with GMRS001 Real-time PCR universal Master Mix (GenePhama, Shanghai, China). The primer sequences are shown in Table S1. Gene expression was quantified using the Comparative C_T Method [22]. In brief, we defined ΔC_T as the C_T of the target gene subtracted from the C_T of the housekeeping gene, glyceraldehyde-3-phosphate dehydrogenase (GAPDH). We further calculated $\Delta\Delta C_T$ as the result of averaged ΔC_T of samples subtracted from the averaged ΔC_T of corresponding genes in INS-1 cells. Assuming a 100% PCR amplification reaction, we defined the ratio of the sample gene expression level relative to the INS-1 cells as $2^{-\Delta\Delta C_T}$.

Electrophysiology. Standard whole-cell recordings were conducted using an EPC-10 patch-clamp amplifier (HEKA, Lambrecht, Germany). Extracellular solution contained the following (in mM): NaCl 130, KCl 2.8, $MgCl_2$ 1.2, Glucose 5, Hepes 10, TEA-Cl 20, $CaCl_2$ 2.6, with pH 7.2. The whole-cell pipette solution contained the following (in mM): CsGlu 110, DMNP–EDTA 5, NaCl 8, $CaCl_2$ 3.6, MgATP 2, GTP 0.3, Hepes 37, and fura-6F 0.2 with pH adjusted to 7.2 using CsOH or HCl. UV-photolysis and membrane capacitance recordings were performed as described previously [20].

Capacitance traces were analyzed as detailed in a previous report [4]. In brief, we fitted the evoked capacitance decay with either a single exponential function, $f(t) = A_0 - A_1 * (1 - \exp(-(t - \tau_0)/\tau_1))$ or a double exponential function, $f(t) = A_0 - A_1 * (1 - \exp(-(t - \tau_0)/\tau_1)) - A_2 * (1 - \exp(-(t - \tau_0)/\tau_2))$, depending on the best quality of the fit. A_1 and A_2 represented the amplitude of the fast and slow endocytosis, while τ_1 and τ_2 were time constants of them. We further divided the amplitudes of both fast and slow endocytosis by the amplitude of prior exocytosis, then normalized to the averaged value in the control cells, and finally summarized as histograms.

Confocal microscopy. To measure transferrin (Tf) internalization, control cells and cells transfected with different shRNAs were bathed in a normal solution containing either Alexa 488- or 568-conjugated Tf (35 μg/ml) at 37 °C for 40 min. All cells were subsequently rinsed, fixed, and observed using confocal microscopy (Fluoview500; Olympus, Japan). The fluorescence of internalized puncta from different *Z* sections were integrated in ImageJ (NIH) as described previously [4].

Data analysis. All data were analyzed using Igor Pro software (Wavemetrics, Lake Oswego, OR). Averaged results are presented as mean values ± SEM with the number of experiments indicated. Statistical significance was evaluated using Student's *t*-test, and asterisks *, **, and *** denote statistical significance with *p*-values less than 0.05, 0.01, and 0.001, respectively.

Results

Identification of Dyn1 in INS-1 cells

In the first systematic profiling of tissue location of different dynamins, Dyn1 was found to be exclusively in the brain and neurons but was absent from organelles, such as the heart, kidney, liver, and pancreas [23]. Although Dyn1 was proposed to function in endocytosis in insulin-secreting cells [24], whether it exists is in these cells is unknown. To address this question, we first used real-time quantitative reverse transcription PCR (RT-PCR) to quantify relative mRNA contents of Dyn1 and Dyn2 in INS-1 cells compared to those in human HEK293 cells and the mouse brain. A sample plot of amplification of the GAPDH gene from INS-1 cells was shown in Fig. S1, in which the C_T value could be determined as the cycle when the fluorescence crossed the threshold from each amplification trace. Averaged ΔC_{T-Dyn1} from INS-1 cells was 17.04 ± 0.35 ($n = 3$), which was much higher than ΔC_{T-Dyn1} ob-

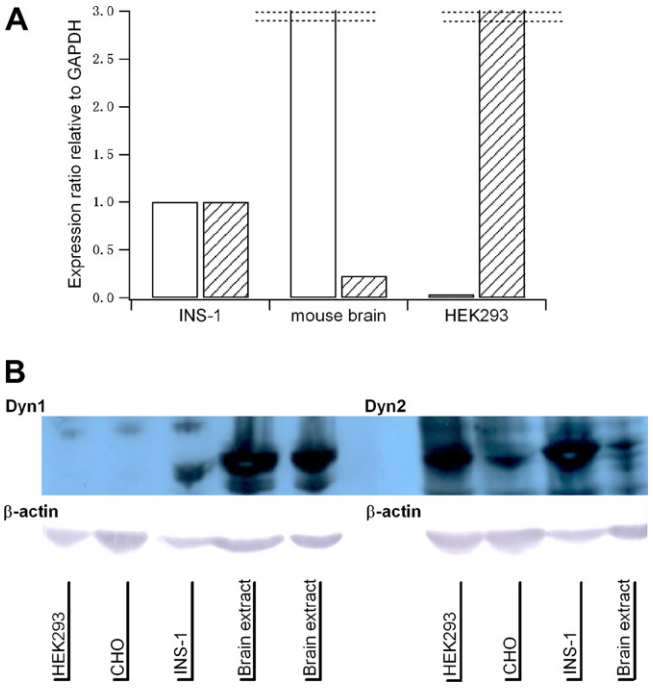

Fig. 1. Identification of Dyn1 and Dyn2 in INS-1 cells. (A) The expression ratios relative to the GADPH from different preparations were plotted from the data listed in Table S1. The ratio of Dyn1 in mouse brain and Dyn2 in HEK293 cells is not completely shown in the plot in order to better visualize differences among ratios from different cells. (B) Western blotting was performed on protein extracts from 10^5 HEK293 cells, CHO cells, INS-1 cells and mouse brain cells with antibodies against either Dyn1 or Dyn2. Dyn1 was enriched in brain extracts but was absent from HEK293 and CHO cells. Abundant Dyn2 was detected in HEK293 cells but was not found in CHO cells or brain samples. However, both Dyn1 and Dyn2 were robustly detected in INS-1 cells. The figure is indicative of two individual experiments.

tained from mouse brain (0.49 ± 0.11, $n = 3$, $p < 0.001$) but was significantly less than that from HEK293 cells (21.83 ± 0.65, $n = 3$, $p < 0.01$). In parallel, averaged ΔC_{T-Dyn2} was largest from mouse brain, smallar from INS-1 cells and smallest from HEK293 cells (Table S2). Subsequently, we quantified the ratio of Dyn1 and Dyn2 expression levels relative to those genes in INS-1 cells. After normalization, as shown in Table S2 and Fig. 1A, we found that Dyn1 was enriched in the mouse brain and Dyn2 was most abundantly expressed in HEK293 cells. Furthermore, the relative expression ratios of Dyn1 and Dyn2 in INS-1 cells were intermediate between those of the brain and HEK293 cells, reflecting the existence of both Dyn1 and Dyn2 mRNA in INS-1 cells.

Next, we tried to determine protein levels of Dyn1 and Dyn2 in INS-1 cells using Western blot experiments. As shown in Fig. 1B, abundant Dyn1 protein was found in brain extracts, while no Dyn1 was detected in either HEK293 or CHO cells. In contrast, Dyn2 was abundant in HEK293 cells but was much less enriched in the mouse brain. These results agreed with a previous report [23] and confirmed the specificity of the antibodies used. Moreover, in agreement with the RT-PCR experiment, robust Dyn1 and Dyn2 protein expression was detected by these antibodies in INS-1 cells (Fig. 1B). Based on these experiments, we conclude that both Dyn1 and Dyn2 are expressed in insulin-secreting INS-1 cells.

Reducing either dynamin isoform affects both fast and slow endocytosis

To address whether different dynamins were involved in distinct endocytosis, we tried to reduce endogenous Dyn1 or Dyn2 expression in INS-1 cells through a gene silencing technique. We generated shRNAs that significantly reduced corresponding gene expression (Fig. 2A), but did not affect the expression of the other isoform (Fig. S2). Homogeneously elevating $[Ca^{2+}]_i$ to a high level (>10 μM) by controlled photolysis led to cells exhibited one or two components of capacitance decay shortly after exocytosis, as showed previously [4]. Reducing Dyn1 expression resulted in an inhibition of fast capacitance decay to 36 ± 7% compared to control

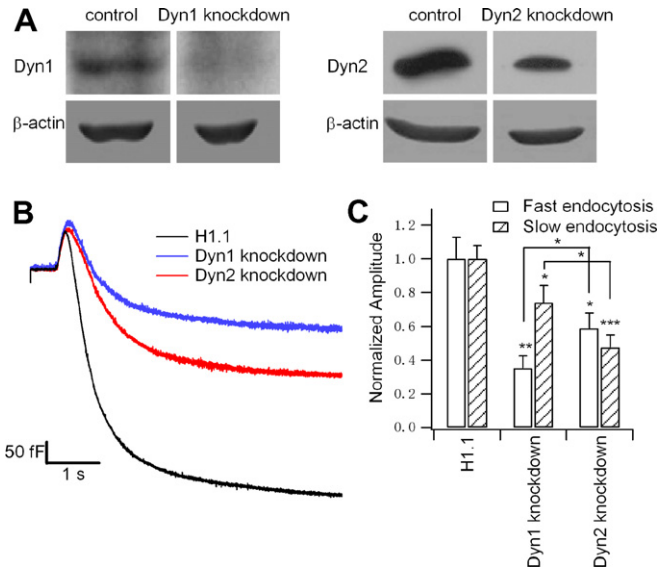

Fig. 2. Dyn1 and Dyn2 simultaneously participate in Ca^{2+}-evoked fast and slow endocytosis. (A) Cells were transfected with shRNAs against Dyn1 (left) and Dyn2 (right), respectively. (B) Averaged Ca^{2+}-evoked capacitance dynamics in control cells transfected with the empty vector (dark, $n = 42$), shRNA against Dyn1 (blue, $n = 29$) and Dyn2 (red, $n = 33$) for 72 h. (C) Effects of knocking down Dyn1 and Dyn2 on fast and slow endocytosis, respectively. Asterisks ∗, ∗∗ and ∗∗∗ denote statistical significances. (For interpretation of the references to color in this figure legend, the reader is referred to the web version of this article.)

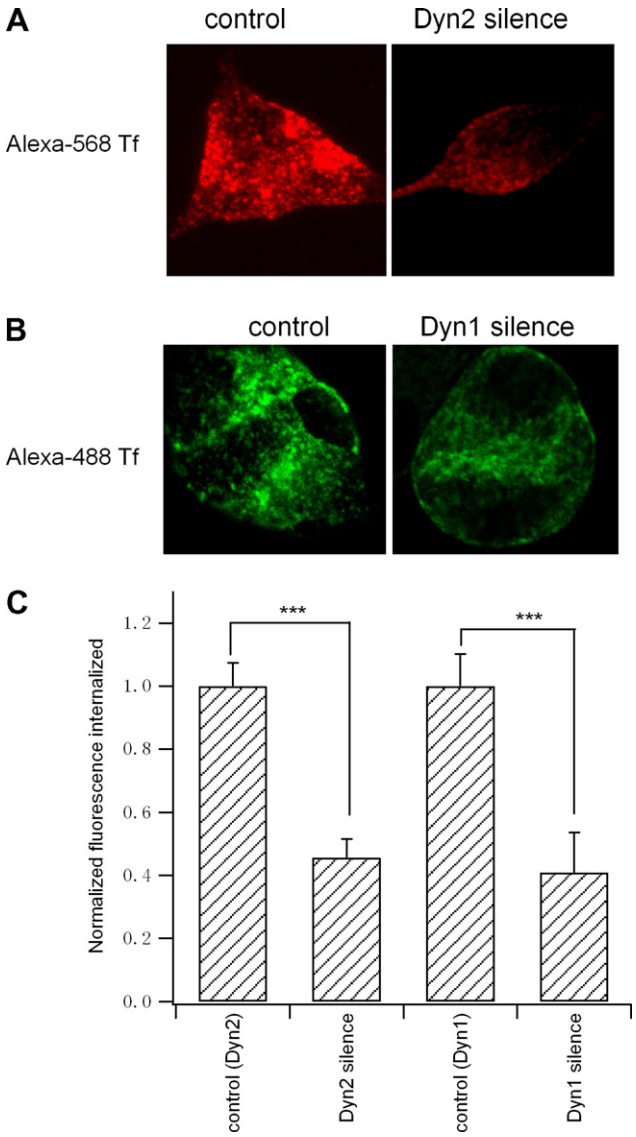

Fig. 3. Inhibition of Tf internalization by Dyn1 or Dyn2 knockdown in INS-1 cells. (A) Control cells expressing the empty pRNAT-H1.1 vector (left) and cells transfected with Dyn2 shRNA (right) were incubated in a solution containing Alexa-568 Tf (35 μg/ml) at 37 °C for 40 min. Example images captured at the middle focal plane are shown here. (B) Control cells (left) and cells transfected with Dyn2 shRNA (right) were incubated in a solution containing Alexa-488 Tf (35 μg/ml) at 37 °C for 40 min. Example images captured at the middle focal plane are shown here. (C) Internalized Tf fluorescence was integrated from different Z planes, normalized to the internalization of Tf in control cells and summarized here. Knocking down either Dyn1 or Dyn2 significantly inhibited Tf internalization, and asterisks ∗∗∗ denote statistical significance ($p < 0.001$) as compared to control.

cells expressing the H1.1 vector alone ($p < 0.01$). However, the slow component was slightly but significantly inhibited as well (74 ± 10%, $p < 0.05$). On the other hand, knocking down Dyn2 also inhibited both the slow (47 ± 7% of the control, $p < 0.05$) and the fast endocytosis (59 ± 9% of the control, $p < 0.001$) (Fig. 2B and C). As we have previously established that fast and slow endocytosis represent clathrin-independent and -dependent endocytosis, respectively [4], we conclude that both Dyn1 and Dyn2 are likely to play redundant roles in these endocytic processes.

Participation of both Dyn1 and Dyn2 in Tf endocytosis

The endocytosis we measured was activated by enhanced Ca^{2+} elevation, which was probably a result of vesicle recycling. To

further probe whether other types of endocytosis were similarly affected or not, we tested the effects of our shRNAs on the internalization of a conventional marker, Tf. Since shRNAs against Dyn2 were tagged with mRFP and shRNAs against Dyn1 were tagged with EGFP, Tf conjugated to probes with different colors were used and different control experiments were performed. After incubating cells with Alexa-488/568 Tf for 40 min, massive internalization was seen in control cells expressing the empty pRNAT-H1.1 vector (Fig. 3A and B). In contrast, cytoplasmic Tf fluorescence was reduced in cells transfected with shRNAs against either Dyn1 or Dyn2. After data pooling and normalization of cells with knocked down Dyn1 expression, Tf internalization was quantified and found to be 41 ±12% ($p < 0.001$) of the endocytosis seen in control cells, whereas the endocytosis was reduced to 46 ± 6% ($p < 0.001$) of the control in cells expressing shRNAs against Dyn2 (Fig. 3C). As Tf internalization is a gold-standard measurement of clathrin-dependent endocytosis, this result further verifies an overlapping role of Dyn1 and Dyn2 in pancreatic β cells.

Overexpressed Dyn1 colocalizes with Dyn2 in INS-1 cells in vivo

It was shown previously that different isoforms of dynamin exhibited differential distribution [23]. However, the colocalization between Dyn1 and Dyn2 was not directly compared in that study. Using confocal microscopy, we examined co-localization of Dyn1 and Dyn2 in quiescent INS-1 cells co-transfecting both Dyn1-EGFP and Dyn2-mRFP. As shown in Fig. 4, most Dyn1 and Dyn2 were found to be colocalized in puncta. Therefore, we argue that Dyn1 and Dyn2 may spatially reside in close proximity to perform overlapped functions.

Discussion

Since Dyn1 is most abundantly found in neuronal and endocrine cells [23], it is hypothesized that Dyn1 specifically regulates the rapid recycling of secretory vesicles, and Dyn2 regulates the slow recycling [3]. The sequence identity between Dyn1 and Dyn2 is highly conserved, with only about 20% of the sequences being divergent from one another. However, among all the domains possessed by dynamin, the PRD domains from Dyn1 and Dyn2 exhibit the most significant differences in sequence (only ~52% homology) [25]. Since the PRD domain plays a crucial role in mediating the interaction of dynamin with various proteins that contain the Src homology (SH3) domain [12], this divergence may contribute to the tissue- and cell-specific function of different dynamins. In fact, different protein interaction sites are predicted for the PRD domain of Dyn1 and Dyn2 [26]. For example, there were two intersectin-binding sites in the PRD domain of Dyn1, while only one site existed in Dyn2. Using surface plasmon resonance technique, it was shown thereafter that the SH3 domain of membrane curvature sensor, amphiphysin, bound to the isolated PRD domains of Dyn1 and Dyn2 with different affinities [26]. Moreover, it is directly demonstrated that the Dyn1 is dephosphorylated at Ser-774 after depolarization in neurons *in vivo* [18]. This dephosphorylation site is crucial to its interaction with syndapin I and is absent from the PRD domain of Dyn2, indicating a clear difference between Dyn1 and Dyn2 in interacting with syndapin I [18]. On top of these experiments, intracellular injection of the pleckstrin homology (PH) domain of Dyn1 specifically inhibited the fast endocytosis in adrenal chromaffin cells, while it was not affected by the PH domain of Dyn2 [19]. In agreement with all these findings, we found that endogenous Dyn1 was preferentially used in fast as compared to slow endocytosis, while the reverse was true for Dyn2 (Fig. 2). This also fits with the results of our previous total internal reflection (TIRF) microscopy experiments, where overexpressed Dyn1 was more likely to be recruited to the clathrin-independent endocytic sites *in vivo*, while the overexpressed Dyn2 was more often associated with clathrin-associated pits [4].

Despite these distinct functional preferences of Dyn1 and Dyn2, we showed that they performed overlapping roles to some extent in different types of endocytosis. In contrast to the specific inhibition of fast endocytosis induced by the intracellular perfusion of Dyn1 antibody or inhibitory peptide in chromaffin cells [3,19], reducing the endogenous level of Dyn1 but not Dyn2 through RNA inference affected both fast and slow endocytosis. Moreover, reducing endogenous levels of either Dyn1 or Dyn2 reduced internalization of Tf in pancreatic β cells, which is a bona fide clathrin-dependent process. Although we cannot completely rule out effects due to non-specific reduction of other proteins induced by our RNA interference experiments, the electrophysiological data coincides with our previous optical experiments; that is, physiologically relevant stimulation recruited both overexpressed Dyn1 and Dyn2 proteins to clathrin-coated pits in live cells [4]. Different cell types could contribute to these different phenomenons observed. Alternatively, antibodies are prone to have non-specific effects, and intracellular perfusion of a domain of the protein leads to interactions that are absent in the full-length protein [18]. During vesicle fission, dynamins are required to form oligomers to recruit accessory proteins and perform the scission. In our study, we showed good colocalization of overexpressed Dyn1 and Dyn2 (Fig. 4), which implies a possible hetero-assembly of Dyn1 and Dyn2 as proposed previously [14]. Nevertheless, we argue that such spatial proximity of different dynamins makes a clean functional separation of these isoforms unlikely. Indeed, overexpressing Dyn2 partially rescued the endocytic blockade during stimulation in synapses from mice knock outs of Dyn1 [27], indicating some extent of functional interchangeability of Dyn1 and Dyn2. From an evolutionary point of view, only one conventional dynamin iso-

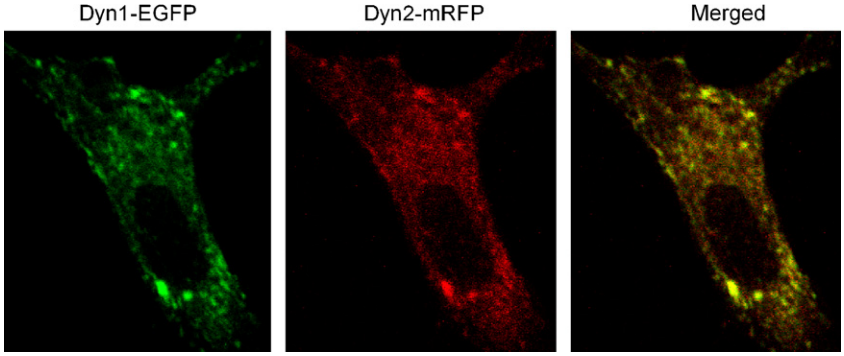

Fig. 4. Colocalization of Dyn1 and Dyn2 overexpressed in INS-1 cells *in vivo*. The INS-1 cell was co-transfected with Dyn1-EGFP and Dyn2-mRFP and observed under a confocal microscope. Only the middle focal plane of the cell is shown here, and the image is representative of 10 similar experiments.

form is found in both *Drosophila* and *Caenorhabditis elegans* [17]. However, both fast and slow synaptic vesicle recycling pathways are present in the retinula synapses of *Drosophila* [28], and enhanced Ca^{2+} elevation evokes two phases of endocytosis in ALA neurons from *C. elegans* [29]. This further supports our argument that Dyn1 and Dyn2 play redundant roles in different endocytic processes *in vivo*, and a clean dissection of distinct vesicle recycling pathways by different dynamin isoforms is not applicable. Therefore, finding other molecules exclusively used in clathrin-independent endocytosis will be the aim of future studies.

In summary, although there are preferences for using either Dyn1 or Dyn2 in clathrin-dependent and -independent endocytosis, we believe that, to a large extent, Dyn1 and Dyn2 perform overlapping roles in pancreatic β cells *in vivo*. Clean dissection and functional evaluation of the clathrin-independent endocytic pathway awaits further exploration.

Acknowledgments

This work was supported by grants from the National Science Foundation of China (30670503, 30670504, and 30630020), a grant from the Beijing Municipal Science & Technology Commission (5072034) and the Major State Basic Research Program of PR China (2006CB70570).

Appendix A. Supplementary data

Supplementary data associated with this article can be found, in the online version, at doi:10.1016/j.bbrc.2008.04.077.

References

[1] S.J. Royle, L. Lagnado, Endocytosis at the synaptic terminal, J. Physiol. 553 (2003) 345–355.
[2] N.C. Harata, A.M. Aravanis, R.W. Tsien, Kiss-and-run and full-collapse fusion as modes of exo-endocytosis in neurosecretion, J. Neurochem. 97 (2006) 1546–1570.
[3] C.R. Artalejo, A. Elhamdani, H.C. Palfrey, Sustained stimulation shifts the mechanism of endocytosis from dynamin-1-dependent rapid endocytosis to clathrin- and dynamin-2-mediated slow endocytosis in chromaffin cells, Proc. Natl. Acad. Sci. USA 99 (2002) 6358–6363.
[4] Z. He, J. Fan, L. Kang, J. Lu, Y. Xue, P. Xu, T. Xu, L. Chen, Ca(2+) triggers a novel clathrin-independent but actin-dependent fast endocytosis in pancreatic beta cells, Traffic (2008).
[5] W.J. Jockusch, G.J. Praefcke, H.T. McMahon, L. Lagnado, Clathrin-dependent and clathrin-independent retrieval of synaptic vesicles in retinal bipolar cells, Neuron 46 (2005) 869–878.
[6] B. Granseth, B. Odermatt, S.J. Royle, L. Lagnado, Clathrin-mediated endocytosis is the dominant mechanism of vesicle retrieval at hippocampal synapses, Neuron 51 (2006) 773–786.
[7] L. He, X.S. Wu, R. Mohan, L.G. Wu, Two modes of fusion pore opening revealed by cell-attached recordings at a synapse, Nature 444 (2006) 102–105.
[8] M. Holt, A. Cooke, M.M. Wu, L. Lagnado, Bulk membrane retrieval in the synaptic terminal of retinal bipolar cells, J. Neurosci. 23 (2003) 1329–1339.
[9] P.E. Macdonald, M. Braun, J. Galvanovskis, P. Rorsman, Release of small transmitters through kiss-and-run fusion pores in rat pancreatic beta cells, Cell Metab. 4 (2006) 283–290.
[10] C. Paillart, J. Li, G. Matthews, P. Sterling, Endocytosis and vesicle recycling at a ribbon synapse, J. Neurosci. 23 (2003) 4092–4099.
[11] H.S. Shpetner, R.B. Vallee, Identification of dynamin, a novel mechanochemical enzyme that mediates interactions between microtubules, Cell 59 (1989) 421–432.
[12] G.J. Praefcke, H.T. McMahon, The dynamin superfamily: universal membrane tubulation and fission molecules?, Nat Rev. Mol. Cell Biol. 5 (2004) 133–147.
[13] A.E. Kruchten, M.A. McNiven, Dynamin as a mover and pincher during cell migration and invasion, J. Cell Sci. 119 (2006) 1683–1690.
[14] Y. Altschuler, S.M. Barbas, L.J. Terlecky, K. Tang, S. Hardy, K.E. Mostov, S.L. Schmid, Redundant and distinct functions for dynamin-1 and dynamin-2 isoforms, J. Cell Biol. 143 (1998) 1871–1881.
[15] P. Rorsman, L. Eliasson, E. Renstrom, J. Gromada, S. Barg, S. Gopel, The cell physiology of biphasic insulin secretion, News Physiol. Sci. 15 (2000) 72–77.
[16] J.D. Orth, M.A. McNiven, Dynamin at the actin–membrane interface, Curr. Opin. Cell Biol. 15 (2003) 31–39.
[17] E.M. Schmid, H.T. McMahon, Integrating molecular and network biology to decode endocytosis, Nature 448 (2007) 883–888.
[18] V. Anggono, K.J. Smillie, M.E. Graham, V.A. Valova, M.A. Cousin, P.J. Robinson, Syndapin I is the phosphorylation-regulated dynamin I partner in synaptic vesicle endocytosis, Nat. Neurosci. 9 (2006) 752–760.
[19] C.R. Artalejo, M.A. Lemmon, J. Schlessinger, H.C. Palfrey, Specific role for the PH domain of dynamin-1 in the regulation of rapid endocytosis in adrenal chromaffin cells, EMBO J. 16 (1997) 1565–1574.
[20] J.G. Duman, L. Chen, A.E. Palmer, B. Hille, Contributions of intracellular compartments to calcium dynamics: implicating an acidic store, Traffic 7 (2006) 859–872.
[21] X. Yang, P. Xu, Y. Xiao, X. Xiong, T. Xu, Domain requirement for the membrane trafficking and targeting of syntaxin 1A, J. Biol. Chem. 281 (2006) 15457–15463.
[22] K.J. Livak, T.D. Schmittgen, Analysis of relative gene expression data using real-time quantitative PCR and the 2(−Delta Delta *C*(T)) Method, Methods 25 (2001) 402–408.
[23] H. Cao, F. Garcia, M.A. McNiven, Differential distribution of dynamin isoforms in mammalian cells, Mol. Biol. Cell 9 (1998) 2595–2609.
[24] M. Hoy, A.M. Efanov, A.M. Bertorello, S.V. Zaitsev, H.L. Olsen, K. Bokvist, B. Leibiger, I.B. Leibiger, J. Zwiller, P.O. Berggren, J. Gromada, Inositol hexakisphosphate promotes dynamin I-mediated endocytosis, Proc. Natl. Acad. Sci. USA 99 (2002) 6773–6777.
[25] F. Soulet, S.L. Schmid, H. Damke, Domain requirements for an endocytosis-independent, isoform-specific function of dynamin-2, Exp. Cell Res. 312 (2006) 3539–3545.
[26] E. Solomaha, F.L. Szeto, M.A. Yousef, H.C. Palfrey, Kinetics of Src homology 3 domain association with the proline-rich domain of dynamins: specificity, occlusion, and the effects of phosphorylation, J. Biol. Chem. 280 (2005) 23147–23156.
[27] S.M. Ferguson, G. Brasnjo, M. Hayashi, M. Wolfel, C. Collesi, S. Giovedi, A. Raimondi, L.W. Gong, P. Ariel, S. Paradise, E. O'Toole, R. Flavell, O. Cremona, G. Miesenbock, T.A. Ryan, P. De Camilli, A selective activity-dependent requirement for dynamin 1 in synaptic vesicle endocytosis, Science 316 (2007) 570–574.
[28] J.H. Koenig, K. Ikeda, Synaptic vesicles have two distinct recycling pathways, J. Cell Biol. 135 (1996) 797–808.
[29] K.M. Zhou, Y.M. Dong, Q. Ge, D. Zhu, W. Zhou, X.G. Lin, T. Liang, Z.X. Wu, T. Xu, PKA activation bypasses the requirement for UNC-31 in the docking of dense core vesicles from *C. elegans* neurons, Neuron 56 (2007) 657–669.